Surface & Coatings Technology 255 (2014) 74–78

Contents lists available at ScienceDirect

Surface & Coatings Technology

journal homepage: www.elsevier.com/locate/surfcoat

# Tribological properties of TiSiN thin films deposited by laser ablation

Iván Camps [a], Stephen Muhl [a], Enrique Camps [b,*], J.G. Quiñones-Galván [b], Martín Flores [c]

[a] Instituto de Investigaciones en Materiales, UNAM, circuito exterior s/n, CU, México DF 04510, Mexico
[b] Departamento de Física, ININ, Apdo. Postal 18-1027, México DF 11801, Mexico
[c] Departamento de Ingeniería de Proyectos, CUCEI, Universidad de Guadalajara, Apdo. Postal 307, CP 45101 Zapopan, Jalisco, Mexico

ARTICLE INFO

Available online 7 January 2014

*Keywords:*
TiSiN
Thin films
Laser ablation
Tribology

ABSTRACT

The simultaneous ablation of silicon and titanium targets in a nitrogen atmosphere was performed in order to obtain the ternary compound TiSiN. The study showed that the plasma density played an important role in determining the composition and properties of the deposited thin films. The plasma parameters were measured using a planar Langmuir probe. The laser fluence applied to the silicon target was varied and this changed the silicon plasma density. The results demonstrated that the deposition rate and the silicon content in the films strongly depended on the plasma density. The composition measurements showed that the silicon content changed from 6 to 29 at.% when the plasma density was increased from $1 \times 10^{19}$ $m^{-3}$ to $1 \times 10^{20}$ $m^{-3}$. The silicon ion energy was fixed at ~160 eV. In order to determine the hardness, friction coefficient, wear resistance and adhesion of the coatings, the TiSiN films were deposited onto nitrided stainless steel substrates at low temperature (200 °C) and a working pressure of 1.33 Pa ($Ar/N_2$ 60/40). The overall results showed that the film hardness varied between 24 and 34 GPa, the friction coefficient (in air) from 0.55 to 0.58 with a wear rate as low as $1.2 \times 10^{-6}$ $mm^3$/N m and the critical load of adhesion, measured by scratch testing, was between 30 and 64 N.

© 2014 Elsevier B.V. All rights reserved.

## 1. Introduction

The idea of improving the hardness of TiN by including a third element which can form a stable oxide, for example Al, Si, or Cr was originally investigated by Hirai et al. [1]. However, the first successful attempts to improve the hardness of TiN by adding silicon were carried out by Shizhi et al. [2] and Veprek et al. [3], using a CVD process, and they reported values of hardness greater than 40 GPa; in the range of the superhard materials. Nevertheless, it is worth noting that the experimental conditions in which those materials were deposited included a toxic atmosphere; Shizi used as reactive gasses $TiCl_4$, $SiCl_4$ and $H_2$, and Veprek used $SiH_4$, moreover, the deposition was carried out at substrate temperatures in the range of 500–600 °C. These experimental conditions can limit the applicability of these types of coatings. One way to avoid such problems is through the use of a reactive PVD process with nitrogen as the reactive gas. The growth of TiSiN thin films by reactive sputtering has been seen to result in polycrystalline samples with mixed phases of TiN, $TiO_2$ and $Si_3N_4$ [4]. Arc evaporation has also been used to deposit TiSiN thin films but in this case many expensive compound Ti–Si targets were needed to obtain a precise control of the Si content in the deposits [5–7]. In order to reduce the substrate temperature, a plasma containing high energy ions (>10 eV) can be used [8]. Finally, various groups have reported that polycrystalline TiN thin films could be deposited using laser ablation of Ti in a nitrogen atmosphere [9,10]. Based on the above considerations we have studied the simultaneous laser ablation of two targets (Ti and Si) in a nitrogen atmosphere to produce TiSiN. We showed in our previous publication [11] that with the correct selection of the Ti ion energy, films of crystalline TiN with either the (111) or (200) crystallographic orientations could be obtained. The relatively high kinetic energy of the ions incident on the substrate during laser ablation means that crystalline deposits can be formed at reduced substrate temperatures, and in the present experiments deposition was carried out at 200 °C. The produced samples were characterized and used to study the tribological behavior of TiSiN.

## 2. Experimental

Fig. 1 shows a schematic representation of the laser ablation system used in this work. It consisted of a vacuum chamber evacuated by a turbomolecular pump to a base pressure of $2.7 \times 10^{-4}$ Pa. During the deposition, the chamber was backfilled with a 60/40 $Ar/N_2$ gas mixture to the working pressure of 1.33 Pa. The laser ablation was performed using a Nd:YAG laser with emission at 1064 nm, a 5 ns pulse duration and a 10 Hz repetition rate. To obtain the thin films of the ternary compound the ablation was carried out simultaneously from two rotating targets (Ti and Si) which were placed perpendicularly to one another; the relative positions of the targets and the substrate are given in Fig. 1. Outside the vacuum chamber the laser beam was divided into two beams of similar intensity; one of the beams was directed onto the titanium target and the other onto the silicon target. The energy

* Corresponding author. Tel.: +52 55 53297200x2251.
*E-mail address:* enrique.camps@inin.gob.mx (E. Camps).

0257-8972/$ – see front matter © 2014 Elsevier B.V. All rights reserved.
http://dx.doi.org/10.1016/j.surfcoat.2013.12.064

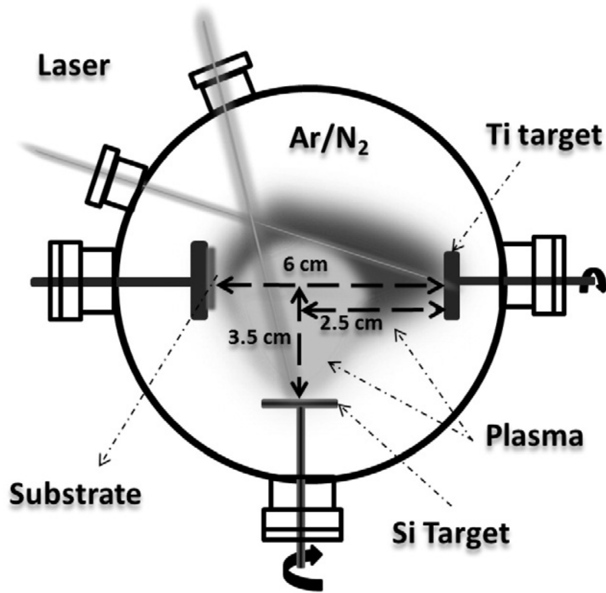


**Fig. 1.** A schematic drawing of the top view of the experimental setup.

fluence (J/cm$^2$) incident on the titanium target was kept constant and the substrate holder was placed 6 cm in front of the titanium target. The distance of the substrate from the source of silicon depended on the position of the ablation point on the silicon target surface and this was varied from 2.5 up to 5 cm. The variation of this distance produced the changes in the silicon plasma density. The laser fluence on the silicon target was varied using attenuators in order to keep the silicon ion energy constant. All the measurements of the silicon plasma characteristics were obtained without ablation of the titanium target and vice versa for the titanium plasma.

The plasma parameters were measured using a 6 mm diameter planar Langmuir probe biased at −50 V such that the ion current to the probe was saturated. The probe current was obtained by measuring the voltage drop across a 15 ohm resistor and was recorded using a Tektronix 500 MHz fast digital oscilloscope. The regimes used for deposition of the films were determined using the Langmuir planar probe placed at the position of the substrate (6 cm from the titanium target). The probe measurements gave time of flight (TOF) curves of the ions and from these using the procedure described by Bulgakova et al. it was possible to calculate the average kinetic energy of the ions, $E_k$, present in the plasma [12]. The calculation uses the following relationship, $\langle E_k \rangle = \frac{mL^2}{2} \frac{\int_0^\infty t^{-2} I(t)dt}{\int_0^\infty I(t)dt}$ where $m$ is the mass of the ion, $L$ is the target to probe distance and $I(t)$ is the probe current.

The plasma density was obtained from the peak values of current of the TOF curves [13].

In this study the experimental conditions were set such that the silicon ion energies were fixed at 160 ± 15 eV and the films were deposited as a function of the plasma density.

Our earlier studies, as well as other published reports have indicated that, even though the ablation was carried out in a gas atmosphere, at the gas pressures used the majority of the ions that are incident on the substrate correspond to ionized target atoms [11,14]. Therefore, in the rest of this work we refer to the silicon and titanium plasmas as the plasma generated by the ablation of the corresponding target and that the ion energies are the energies of the silicon and titanium ions.

Films were deposited at 200 °C on 2.0 cm diameter, 0.5 cm thick, polished AISI 304 stainless steel substrates. In order to enhance the film adhesion the steel substrates were previously nitrided and their hardness was increased to 10 GPa. The details of the nitriding procedure can be found in [15]. No substrate bias was used for these experiments and the substrate holder was connected to ground.

The laser fluence on the titanium target was chosen from previous experiments and was known to give good quality nanocrystalline TiN thin films [11]. Using a laser fluence of 8 J/cm$^2$ on the Ti target, without the silicon ablation, in the argon–nitrogen gas mixture at low temperature, crystalline (111), hard (24 GPa) TiN thin films could be produced. The silicon ablation was included in order to deposit the ternary compound and to study the influence of the inclusion of silicon on the properties of the deposits.

The silicon content of the films, as well as the concentration of other elements, was determined using an EDS Oxford 3608 on a JEOL 5900LV SEM. The normal calibration procedure using Cu and $SiO_2$ standards was carried out before each measurement, but that could mean that there was an undetermined constant error in the absolute values of the elemental concentrations. The crystalline structure of the films was studied by X-ray diffraction (XRD) using a Siemens D-5000 diffractometer with CuKα radiation. The film thickness was determined using a profilometer (KLA Tencor D-120). The hardness measurements were performed using a CSM nanoindenter with a Berkovich indenter, and in these measurements the load was chosen so that the penetration depth did not exceed the 10% of total thickness of the samples. The applied load was varied between 2 and 3 mN, the reported results are the average of ten indentations and the error bars are the standard deviation of these measurements. The adhesion of the films was measured using a Tribotechnic Millenium 100 scratch tester with a 1.58 mm diameter 100Cr6 steel ball (instead of a diamond tip), a loading speed of 100 N/min and a sample movement of 10 mm/min. The wear rate and the friction coefficient were determined from measurements obtained with a CETR UMT reciprocating wear tester, equipped with a polycrystalline polished alumina tip, 10 mm in diameter, with 1 and 2 N loads, 5 Hz of reciprocating movement and 10 mm of displacement amplitude. The reported results are the average of at least three measurements.

## 3. Results

Fig. 2 shows a set of TOF curves of the silicon plasma for some of the regimes used in these experiments. The silicon plasma density was varied from $1 \times 10^{19}$ m$^{-3}$ up to $1 \times 10^{20}$ m$^{-3}$. In the case of the titanium plasma the ion energy and the plasma density were kept constant for all the experiments at 275 eV and $1 \times 10^{20}$ m$^{-3}$, respectively.

The samples were prepared in 2 hour experiments and the average thickness was found to be approximately 600 nm; with a variation of less than 10% for the samples produced at the lowest and highest plasma densities. The thickness of the individual deposits varied by

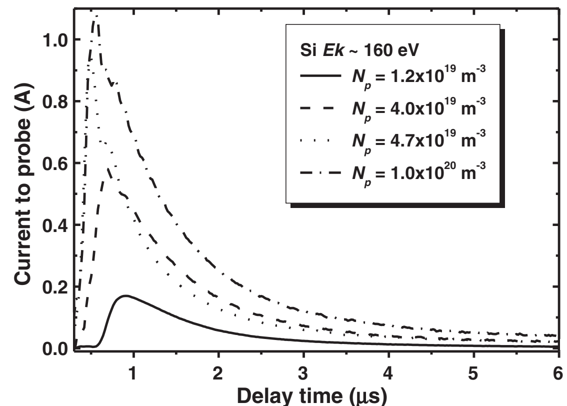


**Fig. 2.** The time of flight (TOF) curves for the silicon plasma for some of the regimes used. $E_k$ is the mean kinetic ion energy and $N_p$ is the value of the plasma density.

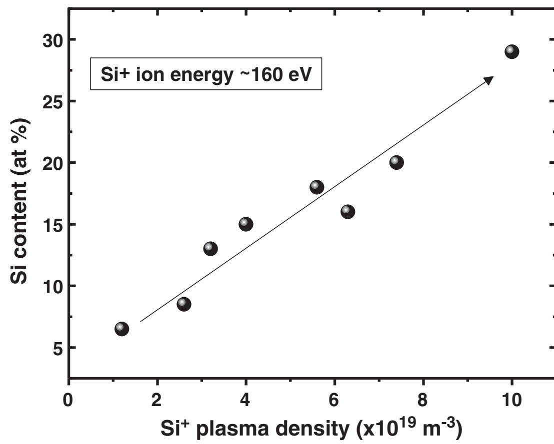


**Fig. 3.** The silicon content of the TiSiN samples as a function of the silicon ion plasma density.

less than ±5% over the surface of the 2.0 cm samples. Fig. 3 shows the increase of silicon content, from 6 to 29 at.%, in the deposited samples as a function of the silicon plasma density. The EDS measurements did not show the presence of oxygen in the films.

The influence of the inclusion of silicon in the films on their structure is shown in Fig. 4. Here we present the XRD patterns for samples made with different values of the silicon plasma density and therefore with different silicon contents. We also show the XRD patterns for a nitrided 304 steel substrate and a sample made without a silicon plasma, i.e. a TiN film oriented in the (111) direction. The peaks from the nitrided substrate can be clearly seen in the TiSiN samples. The overall result shows that the inclusion of silicon produced a reduction in the grain size and a slight shift towards lower 2θ values of the (111) direction of the TiN. No peaks associated with crystalline silicon nitride were observed. These observations are consistent with the idea that the inclusion of silicon promotes the formation of the nc-TiN surrounded by an amorphous phase of the silicon nitride as reported by other groups [16]. However, a conclusive test of this structure was not carried out in this work. Similarly, it is at present not clear if the shift in the peak position is due to the change in the sample composition or changes in the residual stress or a combination of both.

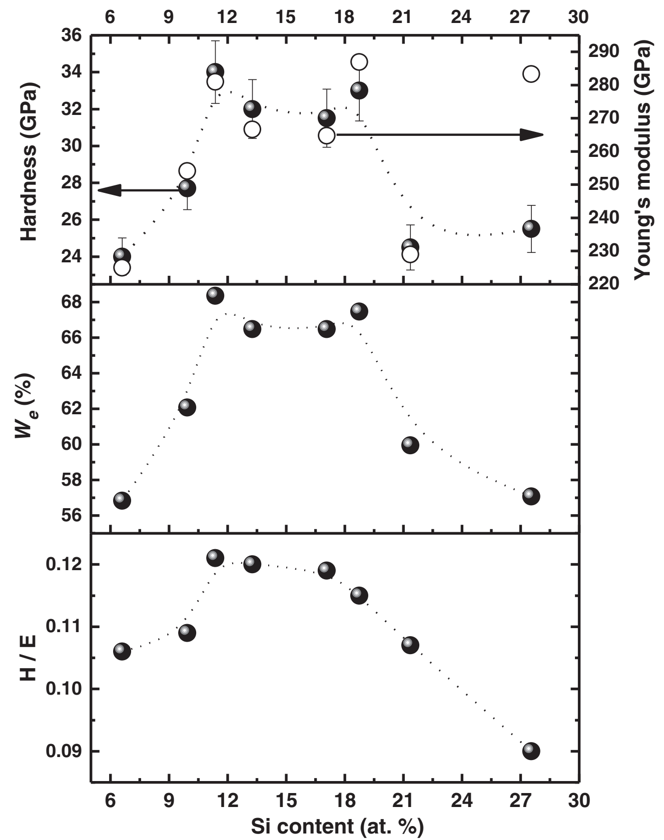


**Fig. 5.** Shown in the upper section is the hardness (■) and Young's modulus E (open circles) as a function of the silicon content of the films, in the middle layer the elastic recovery, $W_e$, also as a function of the silicon content of the films, and in the lower frame the toughness (H/E) of films as a function of the silicon content. The lines are a guide for the eye.

Each of the samples, with different Si contents, was used for the mechanical and tribological tests. The hardness values of the samples deposited at the different plasma densities are presented in Fig. 5; the hardness, H, and the elastic modulus, E, are shown as a function of the

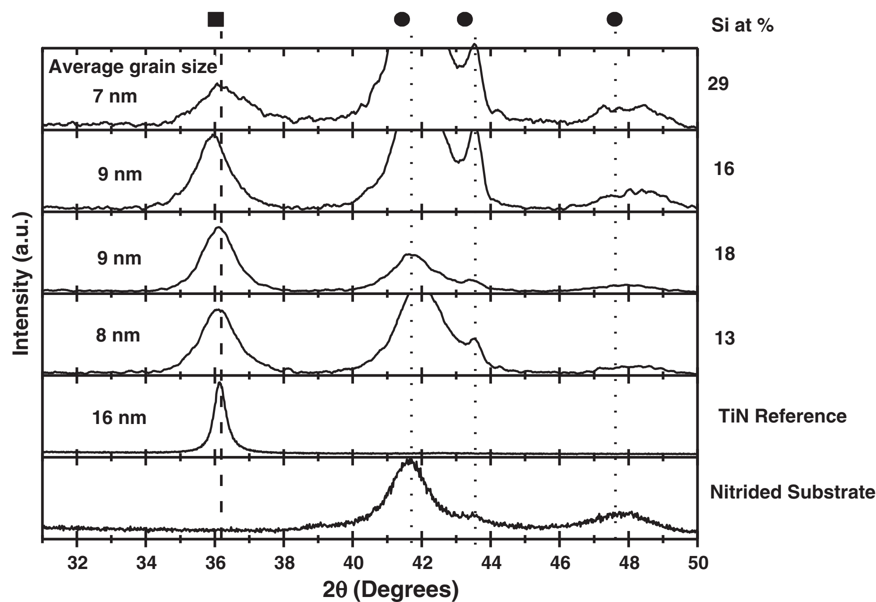


**Fig. 4.** The X-ray diffraction patterns of some of the TiSiN deposited samples at different silicon ion plasma densities. The silicon concentration is given to the right of the graph and the calculated grain size is included on the left-hand side. The TiN reference corresponds to the sample deposited without silicon plasma. The square (■) corresponds to the TiN (111) peak and the circles (●) correspond to the peaks from the nitrided substrate (γ-$Fe_4N$).

silicon content in the films. The maximum hardness, 34 ± 1.5 GPa, was achieved for the middle range of plasma densities and was significantly lower for the highest and lowest plasma densities. In terms of the silicon content, this means that the maximum values of hardness were obtained for silicon concentrations around 13 at.%. This value is somewhat higher than that reported by other authors, for example Hauert and Patscheider [17] reported that various groups had found hardness maxima for silicon concentrations between 5 and 12 at.%, with this variation probably being related to the different procedures used to measure the hardness and the uncertainty in the absolute value of the silicon content. Fig. 5 also shows the calculated elastic recovery, $W_e$, and the toughness of the films expressed by the ratio H/E [18]. Both parameters show a similar behavior as the hardness with the silicon content of the deposits. A recent paper by Musil [19] showed that in general the best nanocomposite coatings have a H/E > 0.1 and a $W_e$ > 60%. Our films, with a silicon content close to 13%, have H/E ≈ 1.2 and $W_e \approx$ 68% indicating that they are of enhanced toughness.

In order to evaluate the adhesion of the films to the steel substrates, scratch tests were performed on the samples measuring the critical load at which complete failure of the coating was observed. The results are presented against the silicon content of the films in Fig. 6, and we have also included a photograph of a typical scratch track. In the photograph we have indicated the different failure modes of the films; the y-axis of the graph, Critical Final Load, corresponds to the failure mode #2 shown in the photograph. The data shows that the best adhesion, critical load ~64 N, was obtained when the Si content was ~13 at.%. Similar to the film hardness, for lower or higher values of Si concentration the failure of the films occurred at lower loads. The lowest critical loads were 30 and 40 N for silicon contents of 6 at.% and 29 at.%, respectively.

For the samples prepared using a plasma density from $1.2 \times 10^{19}$ up to $6.4 \times 10^{19}$ $m^{-3}$ (silicon content between 6 to 18 at.%) the friction coefficient, measured using the reciprocating wear tester at 2 N, was found to decrease from 0.58 to 0.55 but then increased back to 0.58 for the highest plasma density of $1.0 \times 10^{20}$ $m^{-3}$, 29 at.% Si, which is close to the value obtained for the TiN film. The friction coefficient of the nitrided steel substrate was measured under the same experimental conditions and was 0.6.

The wear tracks produced by the reciprocating wear testing were used to calculate the volume of the removed material and therefore the wear rate. The measurements were made at 1 and 2 N loads and the results are shown in Fig. 7 as a function of the silicon content in the samples. In the plot we also show the wear rate for the uncoated nitrided substrate ($2.5 \times 10^{-4}$ $mm^3$ $N^{-1}$ $m^{-1}$) and for the TiN thin film ($3.7 \times 10^{-6}$ $mm^3$ $N^{-1}$ $m^{-1}$). From the plot it can be observed that the lowest values of the wear rate, ~$1.2 \times 10^{-6}$ $mm^3$ $N^{-1}$ $m^{-1}$, were obtained when a plasma density of less than $5 \times 10^{19}$ $m^{-3}$ was used (a silicon content of less than 15 at.%). When higher plasma densities were used the wear rate abruptly increased and there was a strong dependence of the wear rate with the applied load; the higher the load, the higher the wear rate. The wear rate of the TiSiN films produced in this work was much lower than that of nitrided steel and for low Si concentrations the TiSiN films had wear rates similar to those of the TiN films but with a higher hardness.

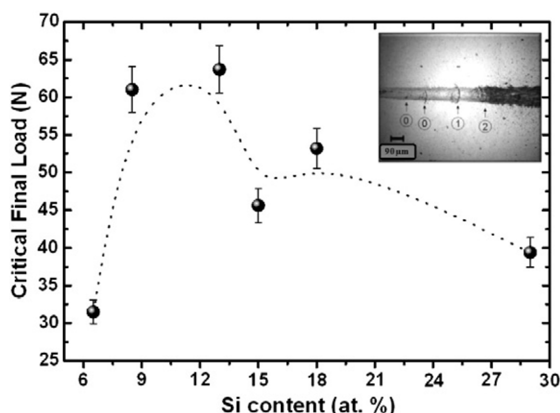


Fig. 6. The scratch test results showing the critical final load as a function of the silicon content of the samples. The inset is a photograph of a typical scratch mark produced during the test; the labels 0, 1 and 2 correspond to individual or isolated events, systematic failures and complete coating delamination, respectively.

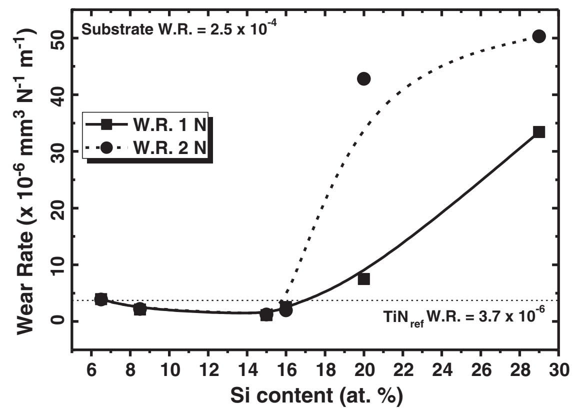


Fig. 7. The wear rate of TiSiN films as a function of their Si content. The lines are a guide for the eye. The wear rates for the nitrided substrate and TiN film are included for comparison.

A possible explanation of the observed mechanical properties, together with the composition and XRD results, is that for the lowest plasma densities the silicon is included as a solid solution within the TiN nanocrystals and that for higher silicon concentrations possibly the TiN nanocrystals are surrounded by a few monolayers of amorphous silicon nitride; as described by other groups [20–22]. The formation of such a structure might be responsible for the observed improvement in the mechanical properties. However, for larger concentrations of silicon the thickness of the amorphous phase could be expected to increase and thus allow mechanical deformation with a corresponding reduction in the hardness and toughness of the deposits.

## 4. Conclusions

In this work TiSiN thin films were produced using the simultaneous ablation of Ti and Si targets in a reactive atmosphere containing nitrogen. The main aim of the present work was to show that by controlling the density of the silicon plasma, while keeping both the Si and Ti ion energies constant as well as the Ti plasma density, it was possible to control the characteristics of the deposits. The results showed that the silicon content in the deposited films was dependent on the plasma density and it was possible to deposit nanocrystalline TiSiN thin films with different silicon contents and different mechanical properties. In particular, we have shown that the hardness, adhesion, coefficient of friction and wear rate are a function of the Si content, although there is some uncertainty in the absolute vales of the Si concentration. The best films at ~13 at.%, had a grain size of ~8 nm, a hardness of ~34 GPa, a H/E ratio of ~0.12, an elastic recovery of ~68%, a critical adhesion load of ~64 N and a wear rate of ~$1.2 \times 10^{-6}$ $mm^3$ $N^{-1}$ $m^{-1}$.

## Acknowledgements

This work was partially supported by CONACYT under contract No. 128732.

## References


[1] T. Hirai, S. Hayashi, J. Mater. Sci. 17 (1982) 1320.
[2] L. Shizhi, S. Yulong, P. Hongrui, Plasma Chem. Plasma Process. 12 (1992) 287.
[3] S. Veprek, S. Reiprich, L. Shizhi, Appl. Phys. Lett. 66 (1995) 2640.

[4] S. Balasubramanian, A. Ramadoss, A. Kobayashi, J. Muthiruland, J. Am. Ceram. Soc. 95 (9) (2012) 2746.
[5] L. Chen, Y. Du, S.Q. Wang, A.J. Wang, H.H. Xu, Mater. Sci. Eng. A 502 (2009) 139.
[6] S. Veprek, M.J.G. Veprek-Heijman, Surf. Coat. Technol. 202 (2008) 5063.
[7] C.L. Chang, W.C. Chen, P.C. Tsai, W.Y. Ho, D.Y. Wang, Surf. Coat. Technol. 202 (2007) 987.
[8] A. Anders, Thin Solid Films 518 (2010) 4087.
[9] J.C.S. Koors, C.J.C.M. Nillesen, S.H. Brongersma, E. van de Riet, J. Dieleman, J. Vac. Sci. Technol. A 10 (1992) 1809.
[10] S.H. Kim, H. Park, K.H. Lee, S.H. Jee, D.J. Kim, Y.S. Yoon, H.B. Chae, J. Ceram. Process. Res. 10 (1) (2009) 49.
[11] L. Escobar-Alarcón, E. Camps, M.A. Castro, S. Muhl, J.A. Mejia-Hernandez, Appl. Phys. A Mater. Sci. Process. 81 (2005) 1221.
[12] N.M. Bulgakova, A.V. Bulgakov, O.F. Bobrenok, Phys. Rev. E. 62 (2000) 5624.
[13] J. Hopwood, C.R. Guarnieri, S.J. Whitehair, J.J. Cuomo, J. Vac. Sci. Technol. A 11 (1993) 152.
[14] J. Bulĩř, M. Novotný, M. Jelínek, L. Jastrabík, Z. Zelinger, Surf. Coat. Technol. 173–174 (2003) 968.
[15] E. Camps, F. Becerril, S. Muhl, O. Alvarez-Fregoso, M. Villagrán, Thin Solid Films 373 (2000) 293.
[16] S. Veprek, S. Reiprich, Thin Solid Films 268 (1995) 64.
[17] R. Hauert, J. Patscheider, Adv. Eng. Mater. 2 (2000) 247.
[18] A. Leyland, A. Matthews, Wear 246 (2000) 1.
[19] J. Musil, Surf. Coat. Technol. 207 (2012) 50.
[20] J. Patscheider, T. Zehndera, M. Diserens, Surf. Coat. Technol. 146–147 (2001) 201.
[21] J. Musil, Surf. Coat. Technol. 125 (2000) 322.
[22] S. Zhang, D. Sun, Y. Fu, H. Du, Surf. Coat. Technol. 198 (2005) 2.